

Potentials of Ni-based bimetallic catalysts supported on zeolite for biokerosene production via catalytic cracking: a mini review

Fatin Oktavianti¹, Aman Santoso¹, and Sumari Sumari^{1*}

¹Department of Chemistry, Faculty of Mathematics and Science, Universitas Negeri Malang, Jl. Semarang No.5, Malang, 65145, Indonesia

Abstract. Aviation, a key global transportation mode, faces increasing demand for sustainable fuels, driving interest in renewable alternatives such as biokerosene derived from biomass. Biokerosene production commonly relies on catalytic hydrodeoxygenation, decarboxylation, and decarbonylation reactions; however, achieving high selectivity toward kerosene-range hydrocarbons remains challenging due to moderate yields, catalyst deactivation, and complex reaction pathways. Nickel-based catalysts are widely investigated for biomass upgrading owing to their hydrogenation activity, while zeolite supports provide acidity and shape selectivity that influence cracking and isomerization reactions. In recent studies, bimetallic Ni-based catalysts supported on zeolites have been explored to modify metal dispersion, acidity, and product distribution. Nevertheless, reported performances vary widely, and in many cases biokerosene yields do not improve relative to monometallic Ni or zeolite-only systems. This review compiles and discusses Ni-based bimetallic zeolite catalysts for biokerosene production, emphasizing observed performance trends, inconsistencies across catalyst formulations and reaction conditions, and the challenges in identifying consistent structure-performance relationships.

1 Introduction

Aviation is vital to the global economy, facilitating the rapid movement of people and goods for tourism, trade, business, and social interactions. The International Air Transport Association (IATA) projects passenger numbers will more than double in the next 20 years, growing at an annual rate of 3.5%, driven by population growth, rising living standards, and lower travel costs. Despite improved fuel efficiency in aviation, carbon emissions continue to rise due to increasing demand. Aviation accounts for around 8% of transportation-related emissions worldwide [1].

Conventional aviation fuel, primarily kerosene derived from crude oil, sees global consumption of approximately 300 million metric tons annually, with demand expected to triple by 2050. The aviation industry aims to reduce CO₂ emissions by 50% by 2050 compared to 2005 levels [2]. To help meet this target, extensive research is underway to develop sustainable aviation fuels (SAFs), including biokerosene, also referred to in the literature as biojet fuel [1].

*Corresponding author: sumari.fmipa@um.ac.id

Biokerosene is produced through the deoxygenation and hydrogenation of triglycerides or fatty acids using heterogeneous bifunctional metal–acid catalysts, and the resulting fuel must comply with international aviation standards such as ASTM D7566 [2]. However, across the reviewed studies, the definition of “biokerosene” varies considerably. Kerosene fractions are reported using different carbon number ranges, including C8-C16 [3-5], C9-C15 [6,7], C10-C13 [8,9], C13-C14 [10], and C11-C12 [11], while several studies report biokerosene-related yields without explicitly specifying the carbon range or calculation basis [12,13].

Catalysts play a central role in biokerosene production by enabling the conversion of biomass-derived feedstocks into hydrocarbons within the desired fuel boiling range. Such conversions commonly rely on heterogeneous bifunctional catalysts, in which metallic sites are responsible for hydrogenation-dehydrogenation steps, while acidic sites promote cracking and isomerization through carbocation-mediated pathways. Effective catalytic performance therefore depends on achieving an appropriate balance between metal and acid functionalities to control chain fragmentation and molecular rearrangement [14]

Ni-based catalysts are widely employed in hydrocarbon upgrading reactions due to their ability to dissociate hydrogen and facilitate hydrogenation reactions. When supported on zeolites, Ni catalysts benefit from the high surface area, well-defined pore structures, and intrinsic acidity of the support, which influence cracking and isomerization behavior. The physicochemical properties of zeolites, including acidity and pore architecture, play an important role in governing reaction pathways and product distribution. Consequently, the interaction between metallic sites and acidic supports is a key factor in determining catalytic activity, selectivity, and stability during biomass-to-fuel conversion processes [14].

Despite the growing number of studies on Ni-based bimetallic catalysts, focused reviews addressing zeolite-supported Ni-based systems for biokerosene production via catalytic cracking remain limited, as existing reviews generally discuss metal catalysts or zeolitic materials in broader contexts. This mini-review therefore summarizes reported behaviors of Ni-based catalysts supported on zeolites, with emphasis on bimetallic systems, while monometallic Ni catalysts are included primarily for comparison. The review is based on literature published mainly within the last ten years, identified using Google Scholar as the primary search platform with access to major publisher databases. The scope is restricted to catalytic cracking routes for biokerosene associated with pyrolysis processes were excluded, even when catalytic terminology was used without clear cracking or hydrogen-assisted conditions. Studies employing non-zeolitic supports or phosphated zeolites (e.g., SAPO materials) are also not considered. As this work is intended as a narrative mini-review rather than a systematic review, no formal meta-analysis or quantitative performance ranking is attempted. Owing to substantial variations in feedstocks, reaction conditions, and biokerosene yield definitions across the selected studies, the discussion is limited to qualitative comparison, highlighting recurring observations, reported trends, and existing inconsistencies, as well as outlining general considerations and open issues for future studies.

2 Discussion

2.1 Zeolite-only system

Zeolites, whether natural or synthetic, are crystalline aluminosilicates with a microporous framework (pore sizes typically $< 10 \text{ \AA}$) built from corner-sharing SiO_4 and AlO_4 tetrahedra. Isomorphous substitution of Si^{4+} by Al^{3+} generates a negatively charged framework that is

charge-balanced by extra-framework cations (commonly alkali or alkaline earth metals) and associated water in the channels, giving the general formula [15]:

$$M_x^{+z}/n[(AlO_2)_x(SiO_2)_y] \cdot nH_2O \quad (1)$$

Catalytic activity in zeolites arises mainly from Brønsted and Lewis acid sites. Brønsted acid sites (BAS) originate from bridging hydroxyl groups (Si–OH–Al) in the framework, acting as strong proton donors that drive key transformations such as alkylation, isomerization, and cracking of hydrocarbons and oxygenates. Lewis acid sites (LAS) are typically associated with extra-framework or coordinatively unsaturated framework aluminum and other metal species, and can be generated by dealumination, metal ion exchange, or heteroatom incorporation. These centers, often octahedrally or trigonally coordinated, accept electron pairs and participate in the polarization and activation of reactants. When BAS and LAS coexist in proximity, they can act cooperatively to form highly active acid ensembles, particularly in dealuminated or metal-modified zeolites.

A combined analysis of zeolite physical properties in Table 1 and catalytic performance and feedstock characteristics in Table 2 reveals that biokerosene yield in zeolite-only systems is governed by a combined effect of acidity strength, pore accessibility, and feedstock molecular structure. In MOR zeolite, the presence of strong Brønsted acid sites together with limited mesoporosity leads to extensive β -scission reactions when processing free fatty acid-rich feedstocks, such as used coconut oil. Although fatty acids are sufficiently small to access internal acid sites, the absence of hydrogen moderation promotes excessive cracking, gas formation, and loss of kerosene-range hydrocarbons, resulting in low biokerosene yields despite moderate conversion. In contrast, H-Beta zeolite exhibits significantly higher biokerosene yields (61-72%), which can be mechanistically attributed to its large mesopore volume and moderate acidity that favor selective deoxygenation over deep cracking. As demonstrated by Sousa et al. [6], triglyceride molecules (~7.5 nm) are too large to enter micropores and therefore react predominantly on external acid sites, where acid strength rather than acid site density controls deoxygenation efficiency. The mesoporous structure reduces diffusion limitations and shortens residence time, suppressing coke formation and secondary cracking. Furthermore, the superior performance observed for hydrolyzed feedstocks compared to intact triglycerides highlights the critical role of feedstock pre-treatment, as hydrogen availability at low pressure is preferentially consumed for deoxygenation and isomerization rather than triglyceride hydrolysis. While ZSM-5, despite possessing the highest total acidity among the studied zeolites, favors extensive cracking and aromatization under low hydrogen pressure due to its strong Brønsted acid sites and microporous framework. This results in high conversion and selectivity but limits kerosene-range preservation, with significant formation of light hydrocarbons (C8-C10) and aromatics reported. Collectively, these results demonstrate that zeolite-only catalysts exhibit an intrinsic trade-off between conversion and selectivity, where feedstock size and functionality dictate accessibility to acid sites, and strong acidity in the absence of metal-assisted hydrogenation inevitably drives product distributions away from the biokerosene window.

Table 1. Physical properties of zeolite.

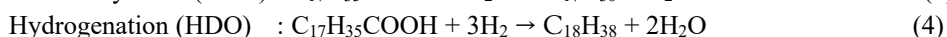
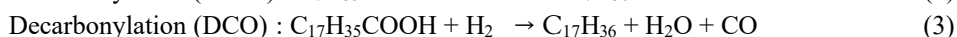
Zeolite	S _{BET} (m ² /g)	Avg. pore diameter (nm)	Pore volume (cm ³ /g)			Acidity (mmol/g)				Ref.
			Micropore	Mesopore	Total	Weak	Medium	Strong	Total	
MOR	328.76	3.51	0.069	0.158	0.227	0.777	-	1.220	1.997	[3]
Hbeta	657.0	5.70	0.130	0.770	0.900	-	-	-	0.586	[6]
ZSM-5	502.55	3.71	-	-	0.470	4.06	3.51	0	7.58	[4]

Table 2. Zeolite catalyst used in biokerosene production.

Feedstock	Content	Zeolite	P (H ₂)	T (°C)	t (hour)	Total yield (%)	Bio-kerosene yield (%)	Content	Selectivity (%)	Ref.
Used coconut oil	Caproic acid (C ₆ H ₁₂ O ₂): 0.40% Caprylic acid (C ₈ H ₁₆ O ₂): 6.24% Capric acid (C ₁₀ H ₂₀ O ₂): 5.87% Lauric acid (C ₁₂ H ₂₄ O ₂): 47.11% Myristic acid (C ₁₄ H ₂₈ O ₂): 17.78% 9,12-Hexadecadienoic acid (C ₁₆ H ₂₈ O ₂): 2.37% Palmitic acid (C ₁₆ H ₃₂ O ₂): 10.33% 9-Octadecenoic acid (C ₁₇ H ₃₂ O ₂): 0.35% 11-Octadecenoic acid (C ₁₈ H ₃₄ O ₂): 7.49% Stearic acid (C ₁₈ H ₃₆ O ₂): 2.06%	MOR	1 atm	350-450	2	17.51	5.89	n/a	49.65	[3]
				450-550			11.62	n/a	57.69	
Palm kernel oil	C8:0: 2.0% C10:0: 2.4% C12:0: 44.6% C14:0: 14.1% C16:0: 10.8% C18:0: 2.3% C18:1: 12.4% C18:2: 0.7% C20:0: 0.1% C20:1: 1.8%	Hbeta	10 bar	350	5	n/a	72	n/a	n/a	[6]
Hydrolyzed olein oil	C12:0: 0.4% C14:0: 0.7% C16:0: 35.1% C16:1: 0.2% C18:0: 5.3% C18:1: 45.5% C18:2: 9.7% C18:3: 0.7% C20:0: 0.7%					n/a	61	n/a	n/a	
Refined palm kernel oil (RPKO)	Lauric acid: 54.70% Myristic acid: 16.27%	ZSM-5	1 atm	600	4	35.36	31.68	Oxygenates: 1.2% Avtur: 16.15%	89.59	[4]

2.2 Ni/zeolite system

Ni-impregnated zeolites are widely applied in biokerosene production because they combine metallic functionality with zeolite acidity to promote oxygen-removal reactions from fatty acid esters, vegetable oils, and bio-oils, yielding hydrocarbons in the biokerosene range. Proper Ni dispersion and controlled acidity influence the balance between desired deoxygenation pathways and excessive cracking. The hydrodeoxygenation process, which includes decarboxylation, decarbonylation, and hydrogenation reactions, is illustrated below [13].



Ni/zeolite catalysts further contribute to hydroisomerization, which is important for generating branched alkanes and improving low-temperature fuel properties. Tuning zeolite acidity and pore architecture helps limit overcracking. In addition, Ni incorporation affects hydrocracking behavior by modifying metal-acid interactions, influencing β -scission reactions and intermediate stabilization on Brønsted acid sites, which can improve overall conversion when properly controlled [7,11,13].

Table 3. Physical properties of catalyst [5].

Catalyst	SBET (m ² /g)	Avg. pore diameter (nm)	Pore volume (cm ³ /g)		Acidity (mmol/g)			
			Micropore	Total	Weak	Medium	Strong	Total
Hbeta	530	-	-	-	0.777	0.189	0.233	0.49
USY	600	-	-	-	0.460	0.511	1.028	2.00
NH ₄ -ZSM-5	330	-	-	-	0.318	0.237	0.744	1.30
10Ni/Hbeta	522	2.27	0.233	0.341	0.273	0.099	0.112	0.48
10Ni/USY	689	1.83	0.235	0.349	0.691	1.277	0.185	2.15
10 Ni/NH ₄ -ZSM-5	324	2.03	0.266	0.150	0.597	0.821	0.422	1.87

Table 4. Ni/zeolite catalyst used in biokerosene production [5].

Feedstock	Zeolite support	% Ni loading	P (H ₂)	T (°C)	t (hour)	Total yield (%)	Biokerosene yield (%)	Content	Selectivity (%)
Palm oil	USY (FAU)	10%	25	425	n/d	n/a	~ 68	n-alkane: 43.59% iso-alkane: 27.92% cyclo-alkane: ~ 12% alkene: - aromatic: ~ 18% oxygenate: -	~ 80
	Hbeta (BEA)						~ 46	n-alkane: ~ 5% iso-alkane: ~ 10% cyclo-alkane: ~ 3% alkene: < 5% aromatic: ~ 80% oxygenate: < 5%	~ 60
	NH ₄ -ZSM-5 (MFI)						~ 39	n-alkane: < 5% iso-alkane: < 5% cyclo-alkane: < 5% alkene: - aromatic: ~ 98% oxygenate: < 5%	~ 65

The incorporation of Ni into zeolite frameworks fundamentally alters catalytic behavior by introducing hydrogen activation and redistributing acid site strength, thereby modifying the balance between deoxygenation, cracking, and aromatization pathways; however, as shown in Tables 3 and 4, the effect of Ni is highly support-dependent and cannot be interpreted independently of pore architecture and residual acidity. Even under identical reaction conditions (425°C and 25 bar H₂), the influence of the zeolite framework on biokerosene production remains pronounced after Ni incorporation. In this context, 10Ni/USY exhibited the highest liquid yield and alkane selectivity, confirming that the FAU structure provides a favorable environment for hydrogen-assisted deoxygenation, where the large pore architecture facilitates access of palm-oil-derived intermediates to Ni metal sites

while moderating acid-catalyzed cracking, ultimately enhancing the formation of n-alkanes and iso-alkanes. In contrast, 10Ni/HBeta showed a marked decrease in alkane selectivity accompanied by dominant aromatic formation, which aligns with previous studies and is confirmed by the authors [25], as the BEA framework intrinsically favors aromatization and, even under high hydrogen pressure, prolonged residence time within its large pores promotes dehydrogenation and cyclization reactions. A similar but more pronounced trend is observed for 10Ni/NH₄-ZSM-5, which produced the highest aromatic content and the lowest alkane fraction due to the strong shape selectivity and high Brønsted acidity of the MFI framework, favoring elimination and aromatization pathways over hydrogenation. Consequently, the poorest performance is observed for 10Ni/NH₄-ZSM-5, where the microporous MFI framework and high residual Brønsted acidity dominate catalytic behavior; despite the presence of Ni, hydrogen spillover is unable to counterbalance strong acid-driven elimination and aromatization pathways, resulting in near-complete aromatic selectivity (~98%) and the lowest biokerosene yield (~39%). Overall, these results demonstrate that Ni enhances biokerosene production only when coupled with supports that provide adequate pore accessibility and moderated acidity, indicating that while Ni introduces hydrogen-assisted deoxygenation pathways absent in zeolite-only systems, optimal performance requires a balanced metal–acid synergy, as exemplified by the Ni/USY catalyst.

2.3 Ni-M/zeolite bimetallic system

The performance of Ni–M/zeolite catalysts in biokerosene production is governed by a complex interplay between acidity, textural accessibility, metal dispersion, and feedstock characteristics, rather than by a single physicochemical parameter. As summarized in Tables 5 and 6, the introduction of a second metal (Mo, Fe, Co, Zn, or Zr) alongside Ni modifies both the acid properties and pore environment of the zeolite support, which in turn controls cracking intensity, deoxygenation pathways, and hydrocarbon distribution.

Across NiMo-based systems, catalytic performance does not scale directly with total acidity or surface area, but instead depends on the accessibility and effective utilization of active sites. This limitation is already apparent in early NiMo/NZ (MOR) systems [26], where relatively high surface area, small crystallite size, and near-theoretical metal loading resulted only in moderate biokerosene yield (~34.8%). The absence of acidity-type differentiation and reaction pathway analysis in this study suggests that surface area alone is insufficient to ensure effective biokerosene selectivity, particularly for MOR zeolites with one-dimensional pore channels that impose diffusion constraints on bulky triglyceride-derived intermediates. More mechanistically resolved studies on NiMo catalysts supported on hierarchical zeolites [27] further demonstrate that catalytic activity does not increase monotonically with acidity. Although NiMo (9:1)/HZ exhibits the highest total acidity, its biokerosene selectivity is lower than that of NiMo (7:3)/HZ and NiMo (8:2)/HZ. This behavior has been attributed to non-uniform metal distribution and partial aggregation at high Ni content, which limits effective reactant-site contact despite increased acidity. In contrast, balanced Ni:Mo ratios promote Mo enrichment on the external surface, leading to the formation of additional external pore structures that enhance accessibility for large triglyceride-derived molecules and improve catalytic selectivity. Collectively, these observations highlight that acid strength and site accessibility, rather than acid quantity alone, govern the catalytic efficiency of NiMo/zeolite systems in biokerosene production.

Similar trends are observed in NiFe- and NiCo-modified ZSM-5 and hierarchical zeolites. Metal impregnation generally reduces BET surface area and total pore volume due to partial pore blockage; however, this does not necessarily impair catalytic performance. Instead, catalysts with optimized metal ratios (e.g., NiCo 8:2) exhibit superior hydrocarbon yields and gasoline-kerosene selectivity compared to those with higher acidity but poorer surface

accessibility. NH₃-TPD analyses indicate that Ni and Co introduce additional Lewis acid sites while preserving Brønsted acidity from the zeolite framework, enabling bifunctional cracking through carbocation intermediates. Excessive acidity or insufficient surface exposure, however, favors overcracking and oxygenate persistence, emphasizing the need for balanced acidity distribution.

Feedstock composition plays a decisive role in interpreting these catalytic trends. Triglyceride-rich oils (coconut oil, jatropha oil, algal oil) require catalysts with sufficient external surface area and mesoporosity to accommodate large molecular sizes, whereas free fatty acid-rich feeds are less diffusion-limited. Studies using algal oil demonstrate that catalysts with higher pore volume and average pore radius (e.g., Ni-Zr/BEA) achieve higher overall conversion but tend to favor heavier fractions (gasoil and residue), indicating insufficient cracking severity. Conversely, Ni-Zr/ZSM-5 systems with smaller pore dimensions promote deeper cracking, shifting selectivity toward gasoline and kerosene fractions at the expense of total liquid yield. These results confirm that pore architecture must be matched to feedstock molecular size to achieve targeted fuel fractions.

Table 5. Physical properties of zeolite.

Catalyst	% Metal loading	SBET (m ² /g)	Acidity (mmol/g)				Ref.
			Weak	Medium	Strong	Total	
Ni-Mo/NZ (MOR)	1.2% Ni; 8.58% Mo	232.18	-	-	-	-	[7]
Ni-Mo/NZ (HEU) (hierarchical zeolite)	5% (Ni:Mo = 9:1)	13.99	-	-	-	1.9517	[12]
	5% (Ni:Mo = 8:2)	22.91	-	-	-	1.1076	
	5% (Ni:Mo = 7:3)	24.62	-	-	-	1.4181	
Ni-Mo/Z	6.72% Ni	33.73	-	-	-	-	[13]
Ni-Fe/ ZSM-5	5% (3.19% Ni; 2.66% Fe)	195.841	-	-	-	-	[8]
	10% (3.75% Ni; 5.43% Fe)	336.617	-	-	-	-	
Ni-Co/NZ (HEU) (hierarchical zeolite)	7.79% Ni; 8.37% Co (Ni:Co = 5:5)	7.63	-	-	-	2.15	[10]
	6.58% Ni; 4.24% Co (Ni:Co = 7:3)	19.13	-	-	-	2.35	
	5.87% Ni; 1.76% Co (Ni:Co = 8:2)	25.13	-	-	-	2.50	
Ni-Zn/MOR	4.5% Ni; 4.5% Zn (0.33% Ni; 1.42% Zn)	-	-	-	-	4.117	[11]
	3% Ni; 6% Zn (1:2)	-	-	-	-	3.972	
	6% Ni; 3% Zn (2:1)	-	-	-	-	4.214	
Ni-Zr/H β	5% Ni; 5% Zr (T red: 500, 600, 700, up to down)	449	1.08	0.74	0.32	2.15	[9]
		449	0.97	1.06	0.56	2.58	
		445	0.87	1.13	0.72	2.71	
Ni-Zr/ZSM-5	5% Ni; 5% Zr	277	1.14	1.19	0.73	3.06	[9]

	(T red: 500, 600, 700, up to down)	271	1.10	0.91	0.88	2.87	
		269	0.66	1.11	0.49	2.26	

Table 6. Ni-M/zeolite catalyst used in biokerosene production.

Feedstock	Catalyst	% Metal loading	P (H ₂)	T (°C)	t (hour)	Total yield (%)	Bio-kerosene yield (%)	Content	Selectivity (%)	Ref.
Renewable diesel (oleic acid)	Ni-Mo/NZ (MOR)	1.2% Ni; 8.58% Mo	1 atm.	375	1.5	84.3	34.77	n/a	36.43	[7]
Jatropha oil	Ni-Mo/NZ (HEU) (hierarchical zeolite)	5% (Ni:Mo = 9:1)	-	375	2	58.59	6.75	n/a	11.52	[12]
		5% (Ni:Mo = 8:2)				58.29	13.324	n/a	22.86	
		5% (Ni:Mo = 7:3)				66.81	14.44	n/a	21.61	
Nyamplung oil (<i>Calophyllum inophyllum</i>)	Ni-Mo/Z	6.72% Ni	12 bar	375	2.5	80.95	3.35	10.71% oxygenate (total)	4.43	[13]
Coconut oil	Ni-Fe/ ZSM-5	5% (3.19% Ni; 2.66% Fe)	30 bar	400	n/a	n/a	~23%	n-Paraffins: - Pentadecane (n-C15): 14.27% - Heptadecane (n-C17): 5.49% Isoparaffins: ~26.93% Olefin: 3.58%	n/a	[8]
		10% (3.75% Ni; 5.43% Fe)						n/a	27.5	
Jatropha oil: Palmitic acid (9.84%) Linoleic acid (33.83%) Oleic acid (37.44%) Stearic acid (15.59%)	Ni-Co/NZ (HEU) (hierarchical zeolite)	7.79% Ni; 8.37% Co (Ni:Co = 5:5)	-	375	2	n/a	n/a	n/a	11.3	[10]
		6.58% Ni; 4.24% Co (Ni:Co = 7:3)						n/a	7.53	
		5.87% Ni; 1.76% Co (Ni:Co = 8:2)						n/a	4.09	
Castor oil: Triglycerides (incl. olefins)	Ni-Zn/MOR	4.5% Ni; 4.5% Zn (0.33% Ni; 1.42% Zn)	-	600 - 1000	n/a	34.72	3.94	Nonene: 0.86% Heptaldehyde: 90.54% 1-heptanol: 1.87% Heptanoic acid: 1.27% 1-undecenoic acid: 4.35% N-nonanal: 1.08%	11.35	[11]
		3% Ni; 6% Zn (1:2)						35.16	4.46	

		6% Ni; 3% Zn (2:1)				37.96	4.04	n/a	10.64	
Algae oil (<i>Spirulina platensis</i>):	Ni-Zr/H β	5% Ni; 5% Zr (T red: 500, 600, 700, up to down)	75	320	2	98	6.35	n/a	6.48	[9]
Triglycerides						94	8.83	n/a	9.39	
FFA						86	9.82	n/a	11.42	
Algae oil (<i>Spirulina platensis</i>):	Ni-Zr/ZSM-5	5% Ni; 5% Zr (T red: 500, 600, 700, up to down)	75	320	2	82	6.55	n/a	7.99	[9]
Triglycerides						86	16.27	n/a	18.92	
FFA						73	12.36	n/a	16.93	

Reaction atmosphere further differentiates catalytic behavior. In the absence of hydrogen, cracking proceeds predominantly via thermal and acid-catalyzed pathways, with oxygen removal occurring mainly through decarboxylation and decarbonylation. Under such conditions, higher acidity directly enhances gasoline-range formation, as observed for Ni-Zn/MOR and NiCo/HZ catalysts. In contrast, hydrogen-assisted systems favor hydrodeoxygenation and alkane stabilization, suppressing oxygenates and enabling improved kerosene selectivity. This explains why catalysts exhibiting high cracking activity without H₂ do not necessarily translate to optimal biokerosene yields under hydrogen-rich conditions.

The collective evidence from Ni-M/zeolite systems indicates that biokerosene production is maximized when moderate-to-strong acidity, accessible pore structures, and well-dispersed bimetallic sites are simultaneously achieved. Excessive acidity, excessive metal loading, or mismatched pore architecture leads to overcracking, aromatization, or poor selectivity. Therefore, catalyst design should prioritize synergistic tuning of bimetallic composition and zeolite structure in accordance with feedstock characteristics and reaction atmosphere, rather than maximizing individual physicochemical parameters.

2.4 Synthesis and characterization of bimetallic catalyst supported on zeolite

The impregnation of active metals onto zeolite frameworks is a crucial step in tailoring catalyst properties for hydrodeoxygenation, hydrogenation, and cracking reactions involved in biokerosene production. The choice of impregnation method significantly affects the catalyst's metal dispersion, particle size, acidity, and overall activity. The most common methods include wet impregnation, incipient wetness, co-impregnation, and sequential impregnation; each offering distinct physicochemical outcomes.

Wet impregnation is a simple and scalable method where zeolite is soaked in a metal precursor solution (e.g., Ni(NO₃)₂·6H₂O), and after drying and calcination, the precursor decomposes into metal oxides or nanoparticles. However, non-uniform metal dispersion may occur depending on precursor concentration and drying conditions, potentially limiting active site accessibility. Incipient wetness impregnation uses a metal precursor solution volume equal to the support pore volume, promoting good dispersion of metal species and small nanoparticles when carefully controlled. However, controlled IWI is not straightforward and requires precise knowledge of pore volume and metal solution properties. Co-impregnation introduces multiple metal precursors simultaneously, promoting metal interaction for improved catalytic activity, reducibility, and coking resistance. This method may enhance hydrogenation-related reactions, although controlling metal distribution and oxidation states remains challenging. Sequential impregnation, on the other hand, introduces metals one by one with intermediate drying, allowing better control over dispersion and interaction, with one metal promoting the other's function where the impregnation sequence can influence metal dispersion and functional synergy.

Once the metal-supported catalysts are prepared, the essential next step is to evaluate their acidity. This property strongly governs catalytic performance, particularly in hydrocracking,

deoxygenation, and isomerization, thereby shaping overall efficiency in biokerosene production. Acidic sites influence the strength and type of surface reactions, product selectivity, and the stability of intermediates. Therefore, an accurate evaluation of both Brønsted and Lewis acid sites is essential to understand the catalyst's functionality. Several techniques are commonly used to measure the acidity of zeolites and their modified forms. One of the simplest quantitative methods to evaluate catalyst acidity is vapor-phase adsorption using a desiccator setup. In this technique, a dried zeolite or catalyst sample is exposed to ammonia or pyridine vapor inside a sealed desiccator for a specific period, allowing the probe molecules to diffuse into the zeolite pores and interact with internal acid sites. Ammonia, acting as both a Brønsted and Lewis base, provides an estimate of the total acidity, while pyridine, which interacts only with Lewis acid sites, is used to identify their specific contribution. A more automated technique is Temperature-Programmed Desorption of Ammonia (NH₃-TPD). In this method, ammonia is first adsorbed onto the catalyst surface at low temperature, and the system is then gradually heated under an inert gas flow. The desorbed ammonia is detected, typically using a thermal conductivity detector (TCD), and the resulting TPD profile indicates total acidity from the integrated desorption area while distinguishing weak, medium, and strong acid sites based on temperature ranges. NH₃-TPD is highly reliable for assessing acidity before and after metal impregnation, as metal addition can neutralize Brønsted sites or generate Lewis acid centers associated with metal oxides. Complementary to this, Fourier Transform Infrared (FTIR) spectroscopy of pyridine adsorption (Py-FTIR) is widely used to differentiate between acid site types. Pyridine selectively binds to Brønsted and Lewis acid sites, producing characteristic IR bands at approximately 1540 cm⁻¹ and 1450 cm⁻¹, respectively. This technique not only quantifies total acidity but also determines the ratio of Brønsted to Lewis sites, a critical factor in balancing cracking and hydrogenation activity in metal-modified zeolites.

In the context of Ni-based bimetallic catalysts supported on zeolites, synthesis methodology plays a decisive role in determining metal dispersion, accessibility of acid sites, and ultimately catalytic selectivity; rather than a universal “best” synthesis route, the literature consistently indicates that the effectiveness of a given method strongly depends on the specific metal pair, support topology, and metal loading level. Across the reviewed studies, incipient wetness and wet co-impregnation remain the most commonly employed techniques due to their simplicity and scalability; however, as clearly demonstrated in Table 7, these conventional methods frequently suffer from non-uniform metal distribution and pore blockage, particularly at higher bimetallic loadings. This limitation is especially pronounced for microporous frameworks such as ZSM-5 and MOR, where sequential or excessive metal deposition leads to significant reductions in BET surface area and pore volume despite increased total metal content. Such textural losses directly restrict reactant diffusion and diminish the effective utilization of acid sites, providing a clear explanation for why higher metal loading does not necessarily translate into higher biokerosene selectivity. For Ni–Mo systems in particular, synthesis-induced dispersion effects are especially critical: as reported for NiMo/MOR catalysts [7], post-impregnation ultrasonication improves Mo dispersion on natural mordenite by preventing Mo aggregation on external surfaces and mitigating pore blockage, whereas alternative energy-assisted methods such as microwave treatment tend to promote Mo clustering, exacerbating pore obstruction and reducing accessibility of internal acid sites. Collectively, these observations underscore that dispersion control, rather than total metal incorporation, governs catalytic effectiveness in Ni–Mo systems, especially for zeolites with one-dimensional pore structures.

In hierarchical zeolite supports, co-impregnation generally yields more favorable outcomes by distributing bimetallic species across both internal and external surfaces. For NiMo and NiCo catalysts supported on hierarchical clinoptilolite [12,10], moderate metal ratios preserve mesoporosity while introducing additional metal-support interfacial sites that

contribute to acidity. Nevertheless, even in hierarchical systems, excessive metal loading leads to mesopore blockage and diminished surface area, underscoring the existence of an optimal loading window rather than a monotonic improvement with metal content.

A recurring pitfall across all bimetallic systems is acid site neutralization following metal impregnation. NH₃-TPD data summarized in Table 7 show that metal addition can either increase apparent total acidity (via the generation of Lewis acid sites) or reduce effective Brønsted acidity through framework interaction or coverage. Importantly, higher total acidity does not consistently correlate with improved biokerosene selectivity. Instead, catalysts exhibiting balanced Brønsted-Lewis acidity and preserved pore accessibility outperform those with higher but less accessible acid site populations. This explains why highly acidic Ni-Zn systems favor extensive cracking toward gasoline-range hydrocarbons [11], whereas moderated acidity in Ni-Zr systems enables better control over cracking severity and fuel-range distribution [9].

Table 7. Recent methods of impregnation of transition metals onto zeolite.

Bimetallic system	% Metal loading	Zeolite support	Impregnation method	T calc. (°C)	Total acidity (mmol/g)	Surface area (S _{BET}) (m ² /g)	Pore size (nm)	Pore volume (cm ³ /g)	Crystal size (nm)	Ref.
Ni-Mo	1.2% Ni; 8.58% Mo	Natural zeolite (mordenite)	Incipient wetness, co-impregnation; ultrasonication	500	n/a	232.18	2.67	0.16	49.35	[7]
Ni-Mo	5% (Ni:Mo = 9:1)	Hierarchical natural zeolite (clinoptilolite)	Co-impregnation	500	1.9517	13.99	11.76	0.0411	n/a	[12]
	5% (Ni:Mo = 8:2)				1.1076	22.91	8.56	0.049	n/a	
	5% (Ni:Mo = 7:3)				1.4181	24.62	7.81	0.048	n/a	
Ni-Mo	6.72% Ni	Zeolite (Merck, unspecified)	n/d	575	n/a	33.73	n/a	n/a	31.8	[13]
Ni-Fe	5% (3.19% Ni; 2.66% Fe)	HZSM-5	Incipient wetness, sequential impregnation; desiccator	550	n/a	195.841	3.07	3.04	n/a	[8]
	10% (3.75% Ni; 5.43% Fe)				n/a	336.617	3.32	2.8	n/a	
Ni-Co	7.79% Ni; 8.37% Co (Ni:Co = 5:5)	Hierarchical natural zeolite (clinoptilolite)	Co-impregnation	500	2.5	7.63	13.09	0.02	n/a	[10]
	6.58% Ni; 4.24% Co (Ni:Co = 7:3)				2.35	19.13	7.93	0.04	n/a	
	5.87% Ni; 1.76% Co (Ni:Co = 8:2)				2.15	25.13	7.11	0.04	n/a	
Ni-Zn	4.5% Ni; 4.5% Zn (0.33% Ni; 1.42% Zn)	Activated natural zeolite (mordenite)	Sequential impregnation; ultrasonication	500	4.117	n/a	n/a	n/a	n/a	[11]
	3% Ni; 6% Zn (1:2)				3.972	n/a	n/a	n/a	n/a	
	6% Ni; 3% Zn (2:1)				4.214	n/a	n/a	n/a	n/a	
Ni-Zr	5% Ni; 5% Zr	HBeta	Wet, co-impregnation	400 (red. 500)	2.15	449	7.2	0.63	Ni = 6; ZrO ₂ = 5	[9]
				400 (red. 600)	2.58	449	6.7	0.62	Ni = 8; ZrO ₂ = 5	
				400 (red. 700)	2.71	445	6.7	0.63	Ni = 13; ZrO ₂ = 6	

Ni-Zr	5% Ni; 5% Zr	ZSM-5	Wet, co- impregnation	400 (red. 500)	3.06	277	2.1	0.06	Ni = 13; ZrO ₂ = 9	[9]
				400 (red. 600)	2.89	171	2.4	0.07	Ni = 14; ZrO ₂ = 10	
				400 (red. 700)	2.26	269	2.4	0.07	Ni = 19; ZrO ₂ = 11	

Despite extensive *ex situ* acidity characterization using NH₃-TPD, many studies still rely on acidity information obtained outside actual reaction environments. In practice, acid site strength and availability may evolve during hydrocracking and deoxygenation due to coke formation, metal oxidation-reduction processes, and water generation. As a result, the limited availability of *operando* or *in situ* acidity data can complicate direct correlations between measured acid properties and observed selectivity trends, particularly in bimetallic systems where metal-acid interactions are sensitive to reaction atmosphere and temperature.

3 Conclusion

Ni-based bimetallic catalysts supported on zeolites have been widely investigated for biokerosene production due to their combined metal functionality and tunable acidic frameworks. The incorporation of a second metal alongside Ni can modify metal dispersion, acidity, and pore accessibility, which in turn influences deoxygenation and cracking behavior. However, comparison across studies reveals that improvements in catalyst complexity do not consistently translate into higher biokerosene yields, as reported performances remain strongly dependent on support type, metal ratio, and reaction conditions.

Current literature shows substantial variability in feedstocks, operating conditions, and product definitions, which limits the establishment of clear structure-performance relationships. In many cases, increased metal loading or bimetallic formulation leads to reduced surface accessibility or pore blockage, offsetting potential benefits from enhanced acidity or metal synergy. These observations indicate that catalyst design for biokerosene production remains highly system-specific rather than governed by universal design rules.

Despite extensive studies on Ni-based bimetallic zeolite catalysts, the lack of standardized reaction conditions and comparable acidity characterization methods remains a major challenge in drawing unified conclusions. Variations in metal dispersion, acidity evolution during reaction, and catalyst stability are rarely evaluated under identical conditions, contributing to the scattered performance trends reported in the literature. Future studies that combine consistent testing protocols with *in-situ* or time-resolved characterization and longer operation periods may help clarify structure-performance relationships and improve the reliability of catalyst design strategies for biokerosene production.

References

1. N. A. A. Qasem, A. Mourad, A. Abderrahmane, Z. Said, O. Younis, K. Guedri, and L. Kolsi, *Journal of Thermal Analysis and Calorimetry* 149, 4287 (2024)
2. C. Tung Chong and J.-H. Ng, *Biojet Fuel in Aviation Applications Production, Usage and Impact of Biofuels*, 1st ed. (Elsevier Science, 2021)
3. A. J. Saviola, K. Wijaya, A. Syoufian, M. F. Vebryana, W. Anggraeni, K. Rozana, N. Darsono, D. A. Saputra, and W. D. Saputri, *Communications in Science and Technology* 9, 356 (2024)

4. W. Trisunaryanti, K. Wijaya, I. Kartini, S. Purwono, R. Rodiansono, A. Mara, and A. S. Rahma, *Reaction Kinetics Mechanisms and Catalysis* 137, 843 (2024)
5. N. Panarmasar, N. Hinchiranan, and P. Kuchonthara, *Materials Today Proceedings* 57, 1082 (2021)
6. F. P. Sousa, L. N. Silva, D. B. de Rezende, L. C. A. de Oliveira, and V. M. D. Pasa, *Fuel* 223, 149 (2018)
7. T. K. Habibie, B. H. Susanto, and M. F. Carli, *E3S Web of Conferences* 67, 2024 (2018)
8. M. A. Muttaqii, F. Kurniawansyah, D. H. Prajitno, and A. Roesyadi, *BULLETIN OF CHEMICAL REACTION ENGINEERING AND CATALYSIS* 14, 309 (2018)
9. Ł. Szkudlarek, K. Chałupka, A. Zimon, M. J. Binczarski, W. Maniukiewicz, P. Mierczyński, and M. I. Szykowska, *Molecules* 29, 5380 (2024)
10. I. Aziz, D. Gustama, T. Retnaningsih, N. Saridewi, L. Adhani, A. A. Dwiatmoko, and M. Ridwan, *RASAYAN Journal of Chemistry* 15, 2026 (2022)
11. A. Santoso, A. B. Saputri, E. Wahyuning, S. Sumari, E. H. Sanjaya, and M. Muntholib, *Reaction Kinetics Mechanisms and Catalysis* 137, 3205 (2024)
12. Aziz, T. Retnaningsih, D. Gustama, N. Saridewi, L. Adhani, and A. A. Dwiatmoko, *AIP Conference Proceedings* (2021)
13. H. Susanto, M. B. Prakasa, and M. H. Shahab, in *IOP Conference Series Materials Science and Engineering* (IOP Publishing, 2016), p. 12009
14. K. A. Sanoja-Lopez, A. M. Balu, H. de Paz Carmona, M. Hájek, R. Luque, and J. M. Hidalgo Herrador, *Chemistry – An Asian Journal* 20, e00635 (2025).
15. B. H. H. Goh, C. T. Chong, H. C. Ong, T. Seljak, T. Kutrašnik, V. Józsa, J.-H. Ng, B. Tian, S. Karmarkar, and V. Ashokkumar, *Energy Conversion and Management* 251, 114974 (2021)